

ENGSCI 711

QUALITATIVE ANALYSIS OF DIFFERENTIAL EQUATIONS

(...and other dynamical systems) Oliver Maclaren
oliver.maclaren@auckland.ac.nz

MODULE OVERVIEW

Qualitative analysis of differential equations (Oliver Maclaren) [[~16-17 lectures/tutorials](#)]

3. Introduction to bifurcation theory [\[4 lectures/tutorials\]](#)

Hyperbolic vs non-hyperbolic systems and structural instability. Various types of bifurcations.
Bifurcation diagrams.

LECTURE 10: BIFURCATION THEORY CONTINUED...CONTINUED

Basic *one-parameter local bifurcation* involving *complex-valued* eigenvalues:

- Hopf bifurcation

1

3

HOPF BIFURCATION

The Hopf bifurcation occurs when a *pair of complex conjugate eigenvalues cross the imaginary axis together*.

Thus at the bifurcation a *a pair of complex conjugate eigenvalues become purely imaginary*

In contrast to before, we now have a non-zero imaginary component and hence have to deal with *oscillatory components*.

(Thus we need the system to have at least dimension two, though the *co-dimension* is still one.)

2

4

HOPF BIFURCATION

A Hopf bifurcation (for our purposes) is characterised by *a change in stability of a fixed point, along with the appearance or the disappearance of a periodic orbit at this fixed point.*

5

HOPF BIFURCATION THEOREM (OR NOT)

Instead we typically a) *find where a pair of complex eigenvalues become purely imaginary* and b) *directly verify that a periodic solution was created/destroyed* (as we pass through the bifurcation) via simulation (or analytical solution in simple cases).

7

HOPF BIFURCATION THEOREM (OR NOT)

There is a *Hopf bifurcation theorem* (See e.g. Glendinning) giving *conditions under which periodic solutions are created/destroyed* as a pair of complex eigenvalues pass through the imaginary axis (and the associated fixed point changes stability)

Unfortunately it is a bit tricky/ugly to verify the conditions for creation/destruction. Though the 'non-zero crossing speed - a *transversality condition* - is not so bad (see later).

6

HOPF BIFURCATION - CO-DIMENSION AGAIN

The Hopf bifurcation occurs in *two-dimensional systems* (or on a two-dimensional reduced/centre manifold of a larger system) BUT

The Hopf bifurcation essentially only *depends on varying one parameter, hence the co-dimension is one.*

8

HOPF BIFURCATION - CANONICAL EXAMPLE

$$\begin{aligned}\dot{x} &= -\omega y + x(\mu - (x^2 + y^2)) \\ \dot{y} &= \omega x + y(\mu - (x^2 + y^2))\end{aligned}$$

HOPF BIFURCATION - CROSSING SPEED

As seen, *a necessary condition for a Hopf bifurcation is finding a pair of complex conjugate eigenvalues crossing the imaginary axis.*

We can also sometimes *verify that this crossing occurs with a non-zero speed* (another necessary condition)

So, we have eigenvalues $\lambda = \pm i\omega$ at critical parameter value
 $\mu = \mu_c$.

and (for a non-degenerate bifurcation) $\frac{\partial \lambda^r}{\partial \mu} \neq 0$ at $\mu = \mu_c$.

where λ^r is the real part of the eigenvalue.

9

11

HOPF BIFURCATION ANALYSIS

Steps

- *Verify* we have a pair of complex conjugate eigenvalues crossing the imaginary axis and an associated change in stability of the fixed point.
- *Verify* (in this example by direct solution, in general via numerical methods) that a periodic orbit exists on one side of the bifurcation.

Note: If a direct solution is possible, then it is typically easiest to construct/verify in polar coordinates.

HOPF BIFURCATION KEY FEATURES

- We call the bifurcation *supercritical* if the emerging/disappearing periodic orbit is stable.
- If it is unstable, we call it *subcritical**^{*}
- The *radius* of the limit cycles grow/shrink continuously from/to zero and proportional to $\sqrt{\mu - \mu_c}$ near μ_c
- The *frequency* of the limit cycle is approximately $\text{Im } \lambda$, evaluated at $\mu = \mu_c$

*Similar terminology is used for other bifurcations (e.g. supercritical pitchfork - stable FP are born).

10

12

HOPF BIFURCATION KEY FEATURES

- The periodic orbit and the fixed point have *opposite stability for the parameter values that they both exist*
- I.e. *supercritical*: stable PO, unstable FP; *subcritical*: unstable PO, stable FP
- Note that it is also *difficult to manually check the theorem conditions* for whether the Hopf bifurcation is 'supercritical' or 'subcritical' (or degenerate).
- Again, it is easier to do it by simulation, direct construction, direct checking etc on a *case-by-case basis*.

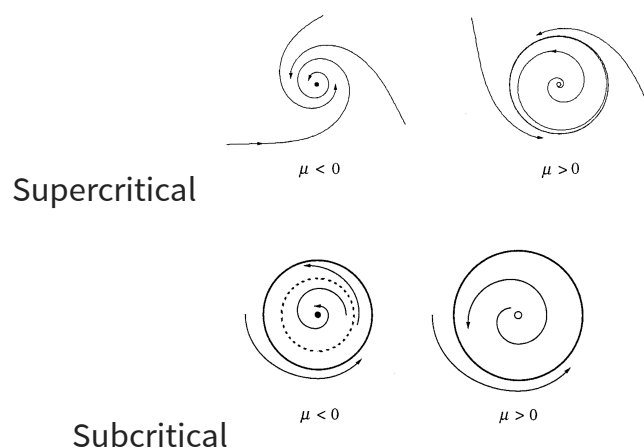
13

FURTHER EXAMPLES

- Saddle-node for periodic orbits
- Homoclinic

15

HOPF BIFURCATION PICTURES



14

EngSci 711 L10 Bifurcation Theory Cont'd.

- o Hopf bifurcation: $\text{Re}(\lambda_i) = 0, \text{Im}(\lambda_i) \neq 0$ at fixed point
 - Basic case
 - Application to chemical oscillator
- o Extras ('collisions' of periodic orbits, global features etc)
 - saddle-node bifurcation of periodic orbits
 - homoclinic bifurcations
- o More applications/extensions?
 - tutorial
 - assignment
 - recommended reading

Example Questions

Exam 2016

(b) Consider the second-order equation

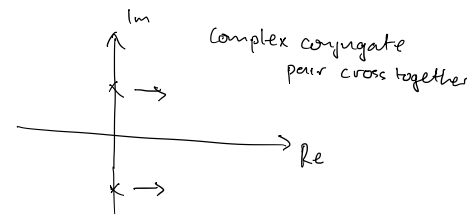
$$\ddot{x} + \mu \dot{x} + (x - x^3) = 0$$

where $x \in \mathbb{R}$ and $\mu \in \mathbb{R}$ is a system parameter.

- (i). Re-write the above equation as system of two first-order equations.
- (ii). Determine a value of μ for which a Hopf bifurcation could potentially occur at the origin. Show all your working.
- (iii). Sketch a bifurcation diagram for a typical supercritical Hopf bifurcation, along with associated typical phase portraits for parameter values before, at and after the critical parameter value. Note: your diagram for this part need not refer to the equation given.

Hopf Bifurcation: creation/destruction of periodic orbits via fixed points

- Two-dimensional state space } went complex eigenvalues
- Still one-parameter bifurcation



- o Purely imaginary ($\text{Re}(\lambda) = 0$) at bifurcation } Key!

Theorem? There is a Hopf bifurcation theorem giving conditions for various possibilities

→ One key condition for a non-degenerate Hopf

$$\left. \frac{d}{du} (\text{Re}(\lambda(u))) \right|_{u=u_c} \neq 0$$

crosses imag. axis at non-zero speed at critical value u_c

→ BUT in general, theorems

- | | |
|--------------------------------|-------------------------------|
| a) convoluted | } see e.g. <u>Glendinning</u> |
| b) hardly ever use in practice | |

Instead, I recommend

- find possible ($\text{Re}(\lambda) = 0, \text{Im}(\lambda) \neq 0$)
- verify directly by numerically investigating either side of bifurcation

In 'exam conditions'
 just find possible,
 maybe check crossing
 speed

Hopf Example

- 'simple' enough to do analytically
- 'Normal form' (generic model of Hopf).

$$\begin{aligned} \textcircled{1} \quad \dot{x} &= -\omega y + x(\mu - (x^2 + y^2)) \\ \dot{y} &= \omega x + y(\mu - (x^2 + y^2)) \end{aligned}$$

or

$$\begin{aligned} \textcircled{2} \quad \dot{r} &= r(\mu - r^2) \quad [\text{polar}] \\ \dot{\theta} &= \omega \end{aligned}$$

$\omega \rightarrow 0$
in bifurcation parameter

Coord. change?

$$\textcircled{1} \rightarrow \textcircled{2}: \text{ either } \begin{cases} ri = x\dot{x} + y\dot{y} \\ r^2\dot{\theta} = x\dot{y} - y\dot{x} \end{cases}$$

or

$$\begin{cases} x = r\cos\theta \\ y = r\sin\theta \\ x+iy = re^{i\theta} \end{cases}$$

(see later)

Consider:

$$\dot{x} = -\omega y + x(\mu - (x^2 + y^2)) \quad \textcircled{1}$$

$$\dot{y} = \omega x + y(\mu - (x^2 + y^2)) \quad \textcircled{2}$$

$\omega > 0$, fixed.

1. Fixed points

$$\textcircled{1} = 0 = -\omega y + x(\mu - (x^2 + y^2))$$

$$\textcircled{2} = 0 = \omega x + y(\mu - (x^2 + y^2))$$

hum... well: try $(0, 0)$.

$$\begin{aligned} 0 &= 0 + 0 & \checkmark \\ 0 &\approx 0, 0 & \checkmark \end{aligned}$$

Others?

→ Nope, since

$$\textcircled{1}: y = \frac{x}{\omega} (\mu - (x^2 + y^2))$$

$$\rightarrow \textcircled{2}: \omega x + \frac{x}{\omega} [\mu - (x^2 + y^2)]^2 = 0$$

$$x \left[\omega + \frac{1}{\omega} []^2 \right] = 0$$

$x \neq 0$ ('others')

But $\omega + \frac{1}{\omega} []^2 > 0$ since $\omega > 0$.

So: $(0, 0)$ only fixed point.

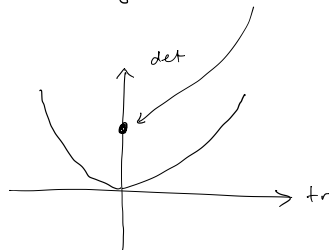
$$2. Df(0,0) = \begin{pmatrix} \mu & -\omega \\ \omega & \mu \end{pmatrix} \quad (\text{verify the long way!})$$

$$\operatorname{tr} = 2\mu$$

$$\det = \mu^2 + \omega^2 > 0$$

$$\lambda^2 - 2\mu\lambda + (\mu^2 + \omega^2) = 0 \Leftrightarrow (\lambda - \mu)^2 + \omega^2 = 0$$

Pure imaginary? Centre!



$$\text{ie } \operatorname{tr} = 0 \Rightarrow \underline{\mu = 0}$$

verify:

$$\left. \begin{aligned} \lambda^2 + \omega^2 &= 0 \\ \lambda &= \pm i\omega \end{aligned} \right\} \text{ when } \mu = 0$$

$$\text{Note } Df(0,0)|_{\mu=0} = \begin{pmatrix} 0 & -\omega \\ \omega & 0 \end{pmatrix}$$

$$\text{so: } \mu = 0 \Rightarrow \lambda = \pm i\omega, \text{ pure imaginary}$$

\Rightarrow Possible Hopf.

$$\begin{aligned} \text{Also: } \lambda &= \mu \pm i\omega \text{ in general} \\ \Rightarrow \underline{\operatorname{Re}(\lambda)} &= \mu, \quad \underline{d\operatorname{Re}(\lambda)/d\mu} = 1 \neq 0 \quad \left. \begin{array}{l} \text{transversality,} \\ \text{non-zero} \\ \text{crossing} \\ \text{speed.} \\ \rightarrow \text{non-degenerate} \end{array} \right\} \end{aligned}$$

In this case we are in normal form

& can analyse analytically what happens

\rightarrow In general, verify numerically

Let's change to polar coord. (fun!)

$$x = r\cos\theta$$

$$y = r\sin\theta$$

$$x+iy = re^{i\theta}, \quad x^2+y^2 = r^2$$

[if I ask, I'll guide through steps --]

$$\frac{d(re^{i\theta})}{dt} = \dot{x} + i\dot{y}$$



$$e^{i\theta} \left[\frac{dr}{dt} + ir \frac{d\theta}{dt} \right] = \omega \underbrace{(-y + ix)}_{-i(x-y)} + (\mu - r^2) \underbrace{(x+iy)}_{re^{i\theta}}$$



$$-i(x-y) = x+iy = re^{i\theta}$$

$$\Rightarrow ix-y = \frac{re^{i\theta}}{-i} = \frac{ire^{i\theta}}{-i^2} = ire^{i\theta}$$

so

$$\cancel{e^{i\theta} [r + ir\dot{\theta}]} = e^{i\theta} ir\omega + (\mu - r^2) re^{i\theta}$$

$$r + ir\dot{\theta} = r(\mu - r^2) + ir\omega$$

equate real & imaginary parts

\Rightarrow

$$\boxed{\begin{aligned} \dot{r} &= r(\mu - r^2) \\ \dot{\theta} &= \omega \end{aligned}}$$

... phenf!

Key point:

$$\begin{cases} \dot{r} = r(\mu - r^2) \\ \dot{\theta} = \omega \end{cases} \quad \leftarrow \text{'like' pitchfork!}$$

(but $r > 0$ & have θ eqn).

where $\begin{cases} r > 0 & (\text{radius}) \\ \omega > 0, \text{ fixed} \\ \mu \text{ control parameter} \end{cases}$

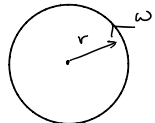
Properties:

$\rightarrow r$ & θ decoupled

$\rightarrow r=0, \omega=0$ (origin) fixed point
 $\xrightarrow{\text{a bit awkward}}$
 \rightarrow as before.

$\rightarrow r^2 = \mu, \omega \neq 0 \Rightarrow \dot{r} = 0, \dot{\theta} \neq 0?$

\Rightarrow circles!



Consider μ variations

Note: if equation has eigenvalue μ at origin

$\mu > 0 \Rightarrow$ unstable } fixed point
 $\mu < 0 \Rightarrow$ stable. } changes stability

Let's do cases

$\mu > 0$

If $\mu = r^2 \Rightarrow$ circles

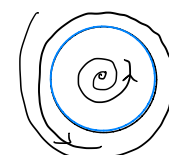
$\circ \mu < r^2 \text{ ie } r^2 > \mu$

$\Rightarrow \dot{r} = r(\mu - r^2) < 0$

$\circ \mu > r^2 \text{ ie } r^2 < \mu$

$\Rightarrow \dot{r} > 0$

So:



- spiral out from origin to circle
- spiral in from outside to circle

$\mu = 0$

radius 'collapses' to origin

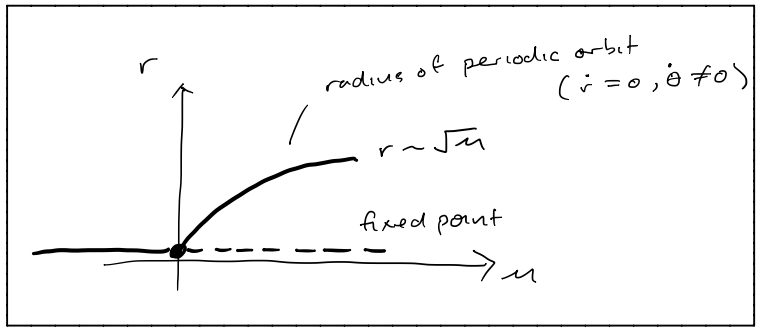
\Rightarrow pure oscillation 'at origin'
 \rightarrow centre!

$\mu < 0$

\Rightarrow no periodic orbit since

$$r^2 \neq \mu < 0$$

Bifurcation diagram : plot key features



Note:

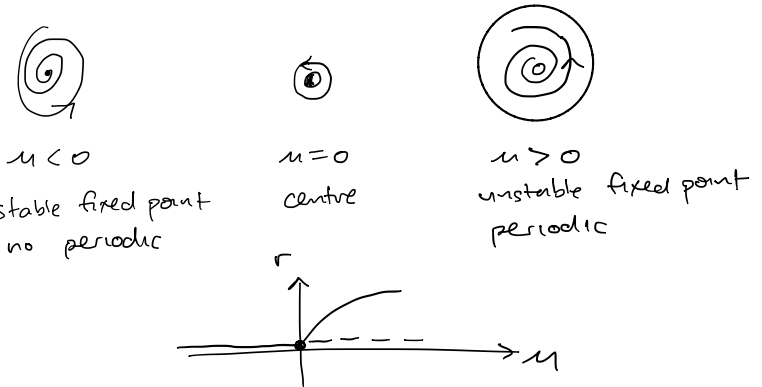
- Fixed point loses stability
- 'Gives birth to' a periodic orbit
- Like pitchfork but $\begin{cases} r > 0 \\ \dot{\theta} \neq 0 \end{cases}$

↳ same terminology:

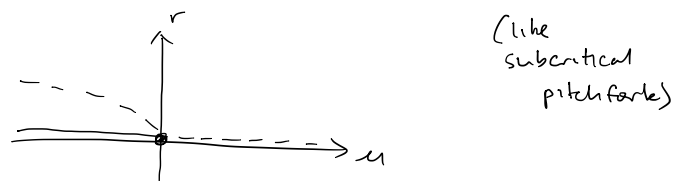
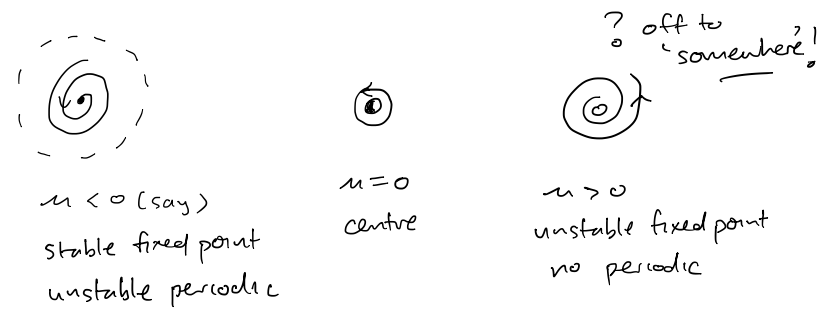
- supercritical (periodic stable)
- subcritical (periodic unstable)

Super vs Sub?

- supercritical : stable periodic appears/disappears via fixed point



- Subcritical : unstable periodic orbit destabilises or stable fixed point
→ dramatic!



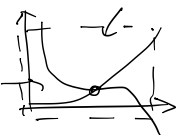
Application

Recall Chlorine - Dioxide - Iodine - Malonic Acid
(CDIMA)
reaction

Model (strogatz 8-3 - attached organ)

$$\begin{aligned}\dot{x} &= a - rx - \frac{4xy}{1+x^2} \\ \dot{y} &= bx \left(1 - \frac{y}{1+x^2}\right)\end{aligned}$$

→ we found trapping region:



→ need to verify/check when fixed point is unstable

→ turns out this is a Hopf bifurcation case

Details: attached
+ XPPaut demonstration.

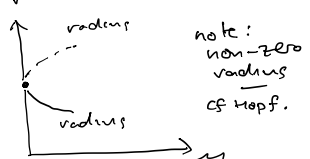
- Extras (typically analyse periodic orbits/global etc via maps)

Saddle-node periodic

'collision' of / 'birth of' pair of stable & unstable periodic orbits

→ like SN but periodic orbits instead of fixed points

Typical bif. diagram

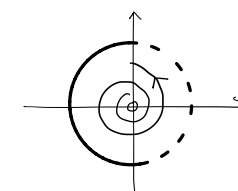
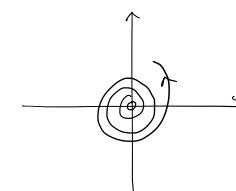


Example (see eg Perko 4.5, example 2)

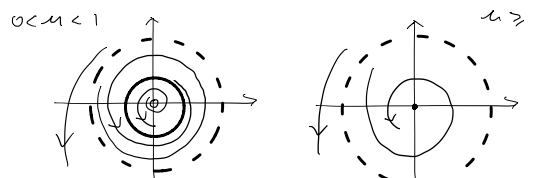
eg

$$\begin{cases} \dot{r} = -r[m - (r^2 - 1)^2] \\ \dot{\theta} = \omega \end{cases}$$

$m < 0$ $m = 0$



stable & unstable periodic orbits 'appear/disappear' together 'out of nowhere' → away from the fixed point



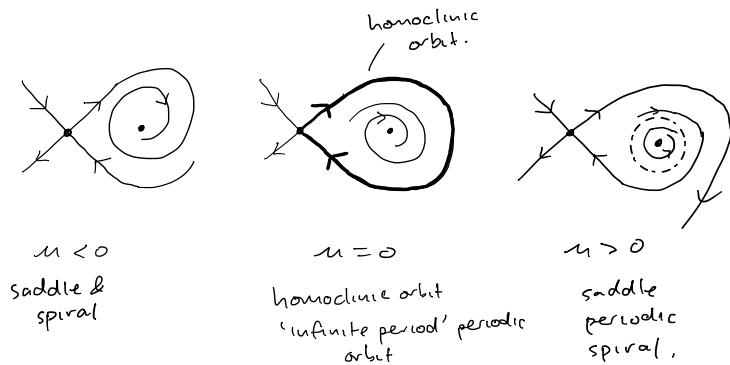
unstable & stable periodic orbits separate

stable periodic disappears at origin via Hopf. (local to fixed point)

• Extras

Homoclinic bifurcation (truly 'global')

- unstable & stable manifolds 'collide'
- ('large amplitude' ($r \neq 0$) periodic orbit appears/disappears)
- re periodic orbit 'collides' with saddle point's manifolds



Example (Strogatz section 8.4)

$$\begin{cases} \dot{x} = y \\ \dot{y} = my + x - x^2 + xy \end{cases}$$

→ see attached.

even more: see attached

Example 2 (A Saddle-Node Bifurcation at a Nonhyperbolic Periodic Orbit). Consider the planar system

$$\begin{aligned}\dot{x} &= -y - x[\mu - (r^2 - 1)^2] \\ \dot{y} &= x - y[\mu - (r^2 - 1)^2]\end{aligned}$$

which is of the form of equation (5) in Section 4.4. Writing this system in polar coordinates yields

$$\begin{aligned}\dot{r} &= -r[\mu - (r^2 - 1)^2] \\ \dot{\theta} &= 1.\end{aligned}$$

For $\mu > 0$ there are two one-parameter families of periodic orbits

$$\Gamma_\mu^\pm: \gamma_\mu^\pm(t) = \sqrt{1 \pm \mu^{1/2}}(\cos t, \sin t)^T$$

with parameter μ . Since the origin is unstable for $0 < \mu < 1$, the smaller limit cycle Γ_μ^- is stable and the larger limit cycle Γ_μ^+ is unstable. For $\mu = 0$ there is a semistable limit cycle Γ_0 represented by $\gamma_0(t) = (\cos t, \sin t)^T$. The phase portraits for this system are shown in Figure 1 and the bifurcation diagram is shown in Figure 2. Note that there is a supercritical Hopf bifurcation at the origin at the bifurcation value $\mu = 1$.

In Example 2 the points $r_\mu^\pm = \sqrt{1 \pm \mu^{1/2}}$ are fixed points of the Poincaré map $P(r, \mu)$ of the periodic orbit $\gamma_0(t)$ along any ray from the origin

$$\Sigma = \{x \in \mathbb{R}^2 \mid r > 0, \theta = \theta_0\};$$

i.e., we have $d(\sqrt{1 \pm \mu^{1/2}}, \mu) = 0$ where $d(r, \mu) = P(r, \mu) - r$ is the displacement function. The bifurcation diagram is given by the graph of the relation $d(r, \mu) = 0$ in the (μ, r) -plane. Using equation (2), we can compute the derivative of the Poincaré map at $r_\mu^\pm = \sqrt{1 \pm \mu^{1/2}}$:

$$DP(\sqrt{1 \pm \mu^{1/2}}, \mu) = e^{\pm 8\mu^{1/2}(1 \pm \mu^{1/2})\pi},$$

cf. Problem 2. We see that for $0 < \mu < 1$, $DP(\sqrt{1 - \mu^{1/2}}, \mu) < 1$ and $DP(\sqrt{1 + \mu^{1/2}}, \mu) > 1$; the smaller limit cycle is stable and the larger limit cycle is unstable as illustrated in Figures 1 and 2. Furthermore, for $\mu = 0$ we have $DP(1, 0) = 1$, i.e., $\gamma_0(t)$ is a nonhyperbolic periodic orbit with both of its characteristic exponents equal to zero.

Remark 1. In general, for planar systems, the bifurcation diagram is given by the graph of the relation $d(s, \mu) = 0$ in the (μ, s) -plane where

$$d(s, \mu) = P(s, \mu) - s$$

is the displacement function along a straight line Σ normal to the nonhyper-

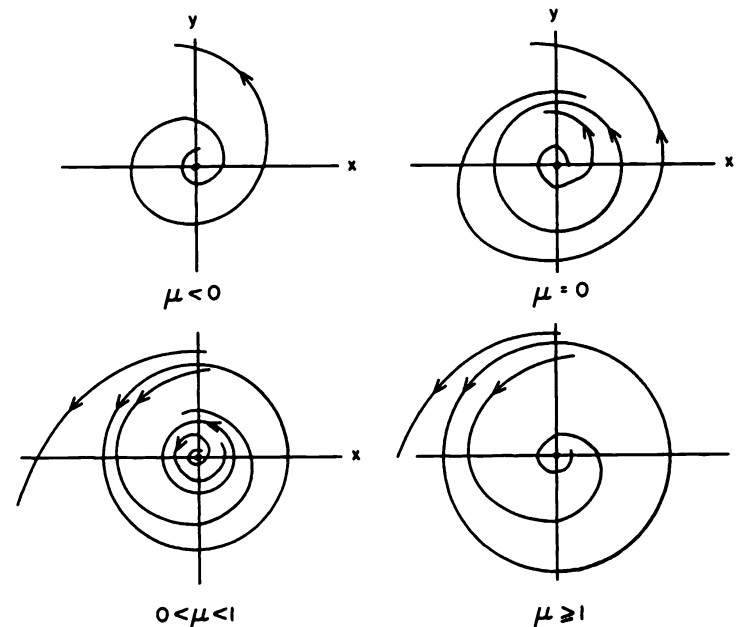


Figure 1. The phase portraits for the system in Example 2.

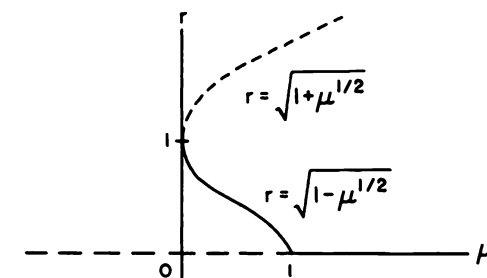


Figure 2. The bifurcation diagram for the saddle-node bifurcation at the nonhyperbolic periodic orbit $\gamma_0(t)$ of the system in Example 2.

bolic periodic orbit Γ_0 at x_0 . We take s to be the signed distance along the straight line Σ , with s positive at points on the exterior of Γ_0 and negative at points on the interior of Γ_0 , as in Figure 3 in Section 3.4 of Chapter 3.

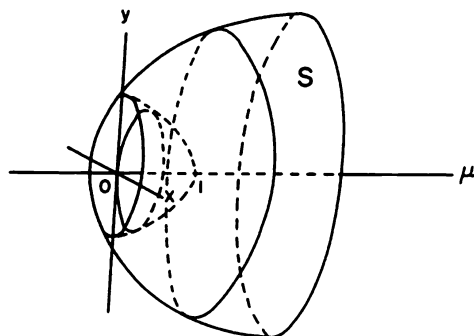


Figure 3. The one-parameter family of periodic orbits S of the system in Example 2.

In this context, it follows that for each fixed value of μ , the values of s for which $d(s, \mu) = 0$ define points x_j on Σ near the point $x_0 \in \Gamma_0 \cap \Sigma$ through which the system (1) has periodic orbits $\gamma_j(t) = \phi_t(x_j)$. For example, in Figure 2, each vertical line $\mu = \text{constant}$, with $0 < \mu < 1$, intersects the curve $d(r, \mu) = 0$ in two points $(\mu, \sqrt{1 \pm \mu^{1/2}})$; and the system in Example 2 has periodic orbits $\gamma_\mu^\pm(t)$ through the points $(\sqrt{1 \pm \mu^{1/2}}, 0)$ on the x -axis in the phase plane. As in Figure 2 in Section 4.4, each one-parameter family of periodic orbits generates a surface S in $\mathbb{R}^2 \times \mathbb{R}$. For example, the periodic orbits of the system in Example 2 generate the surface S shown in Figure 3. Since in general there is only one surface generated at a saddle-node bifurcation at a nonhyperbolic periodic orbit, we regard the two one-parameter families of periodic orbits (with parameter μ) as belonging to one and the same family of periodic orbits. In this case, we can always define a new parameter β (such as the arc length along a path on the surface S) so that $\Gamma_{\mu(\beta)}$ defines a one-parameter family of periodic orbits with parameter β .

Example 3 (A Transcritical Bifurcation at a Nonhyperbolic Periodic Orbit). Consider the planar system

$$\begin{aligned}\dot{x} &= -y - x(1 - r^2)(1 + \mu - r^2) \\ \dot{y} &= x - y(1 - r^2)(1 + \mu - r^2).\end{aligned}$$

In polar coordinates we have

$$\begin{aligned}\dot{r} &= -r(1 - r^2)(1 + \mu - r^2) \\ \dot{\theta} &= 1.\end{aligned}$$

For all $\mu \in \mathbb{R}$, this system has a one-parameter family of periodic orbits

represented by

$$\gamma_0(t) = (\cos t, \sin t)^T$$

and for $\mu > -1$, there is another one-parameter family of periodic orbits represented by

$$\gamma_\mu(t) = \sqrt{1 + \mu}(\cos t, \sin t)^T.$$

The bifurcation diagram, showing the transcritical bifurcation that occurs at the nonhyperbolic periodic orbit $\gamma_0(t)$ at the bifurcation value $\mu = 0$, is shown in Figure 4. Note that a subcritical Hopf bifurcation occurs at the nonhyperbolic critical point at the origin at the bifurcation value $\mu = -1$.

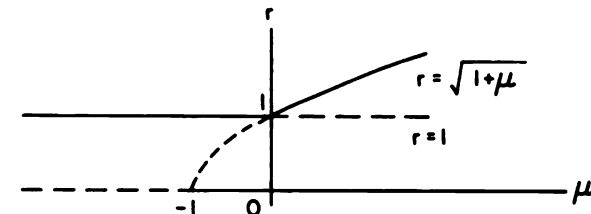


Figure 4. The bifurcation diagram for the transcritical bifurcation at the nonhyperbolic periodic orbit $\gamma_0(t)$ of the system in Example 3.

In Example 3 the points $r_\mu = \sqrt{1 + \mu}$ and $r_\mu = 1$ are fixed points of the Poincaré map $P(r, \mu)$ of the nonhyperbolic periodic orbit Γ_0 ; i.e., we have

$$d(\sqrt{1 + \mu}, \mu) = 0$$

for all $\mu > -1$ and

$$d(1, \mu) = 0$$

for all $\mu \in \mathbb{R}$ where $d(r, \mu) = P(r, \mu) - r$. Furthermore, using equation (2), we can compute

$$DP(\sqrt{1 + \mu}, \mu) = e^{-4\mu(1+\mu)\pi}$$

and

$$DP(1, \mu) = e^{4\mu\pi},$$

cf. Problem 2. This determines the stability of the two families of periodic orbits as indicated in Figure 4. We see that $DP(1, 0) = 1$; i.e., there is a nonhyperbolic periodic orbit Γ_0 with both of its characteristic exponents equal to zero at the bifurcation value $\mu = 0$. In this example, there are two distinct surfaces of periodic orbits, a cylindrical surface and a parabolic surface, which intersect in the nonhyperbolic periodic orbit Γ_0 ; cf. Problem 3.

Example 4 (A Pitchfork Bifurcation at a Nonhyperbolic Periodic Orbit). Consider the planar system

$$\begin{aligned}\dot{x} &= -y + x(1 - r^2)[\mu - (r^2 - 1)^2] \\ \dot{y} &= x + y(1 - r^2)[\mu - (r^2 - 1)^2].\end{aligned}$$

In polar coordinates we have

$$\begin{aligned}\dot{r} &= r(1 - r^2)[\mu - (r^2 - 1)^2] \\ \dot{\theta} &= 1.\end{aligned}$$

For all $\mu \in \mathbb{R}$, this system has a one-parameter family of periodic orbits represented by

$$\gamma_0(t) = (\cos t, \sin t)^T$$

and for $\mu > 0$ there is another family (with two branches as in Remark 1) represented by

$$\gamma_\mu^\pm(t) = \sqrt{1 \pm \mu^{1/2}}(\cos t, \sin t)^T.$$

Using equation (2) we can compute

$$DP(\sqrt{1 \pm \mu^{1/2}}, \mu) = e^{4\mu(1 \pm \mu^{1/2})\pi}$$

and

$$DP(1, \mu) = e^{-4\pi\mu}.$$

This determines the stability of the two families of periodic orbits as indicated in Figure 5(a). We also see that $DP(1, 0) = 1$; i.e., there is a

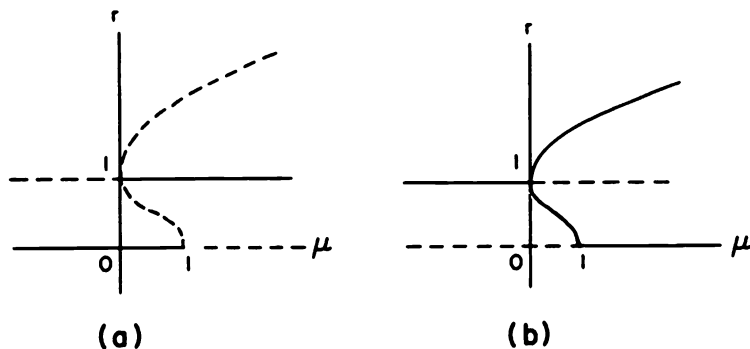


Figure 5. The bifurcation diagram for the pitchfork bifurcation at the nonhyperbolic periodic orbit $\gamma_0(t)$ of the system (a) in Example 4 and (b) in Example 4 with $t \rightarrow -t$.

nonhyperbolic periodic orbit Γ_0 with both of its characteristic exponents equal to zero at the bifurcation value $\mu = 0$. Note that a Hopf bifurcation occurs at the nonhyperbolic critical point at the origin at the bifurcation value $\mu = 1$. Also, note that if we reverse the sign of t in this example, i.e., let $t \rightarrow -t$, then we reverse the stability of the periodic orbits and we would have the bifurcation diagram with a pitchfork bifurcation shown in Figure 5(b).

Using the implicit function theorem, conditions can be given on the derivatives of the Poincaré map which imply the existence of a saddle-node, transcritical or pitchfork bifurcation at a nonhyperbolic periodic orbit of (1). We shall only give these conditions for planar systems. In the next theorem $P(s, \mu)$ denotes the Poincaré map along a normal line Σ to a nonhyperbolic periodic orbit Γ_0 at a bifurcation value $\mu = \mu_0$ in (1). As in Section 4.2, D denotes the partial derivative of $P(s, \mu)$ with respect to the spatial variable s .

Theorem 1. Suppose that $f \in C^2(E \times J)$ where E is an open subset of \mathbb{R}^2 and $J \subset \mathbb{R}$ is an interval. Assume that for $\mu = \mu_0$ the system (1) has a periodic orbit $\Gamma_0 \subset E$ and that $P(s, \mu)$ is the Poincaré map for Γ_0 defined in a neighborhood $N_\delta(0, \mu_0)$. Then if $P(0, \mu_0) = 0$, $DP(0, \mu_0) = 1$,

$$D^2P(0, \mu_0) \neq 0 \quad \text{and} \quad P_\mu(0, \mu_0) \neq 0, \quad (3)$$

it follows that a saddle-node bifurcation occurs at the nonhyperbolic periodic orbit Γ_0 at the bifurcation value $\mu = \mu_0$; i.e., depending on the signs of the expressions in (3), there are no periodic orbits of (1) near Γ_0 when $\mu < \mu_0$ (or when $\mu > \mu_0$) and there are two periodic orbits of (1) near Γ_0 when $\mu > \mu_0$ (or when $\mu < \mu_0$). The two periodic orbits of (1) near Γ_0 are hyperbolic and of the opposite stability.

If the conditions (3) are changed to

$$\begin{aligned}P_\mu(0, \mu_0) &= 0 \quad DP_\mu(0, \mu_0) \neq 0 \quad \text{and} \\ D^2P(0, \mu_0) &\neq 0,\end{aligned} \quad (4)$$

then a transcritical bifurcation occurs at the nonhyperbolic periodic orbit Γ_0 at the bifurcation value $\mu = \mu_0$. And if the conditions (3) are changed to

$$\begin{aligned}P_\mu(0, \mu_0) &= 0, \quad DP_\mu(0, \mu_0) \neq 0 \\ D^2P(0, \mu_0) &= 0 \quad \text{and} \quad D^3P(0, \mu_0) \neq 0,\end{aligned} \quad (5)$$

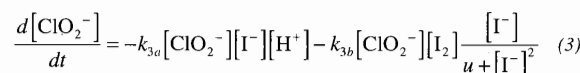
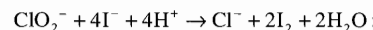
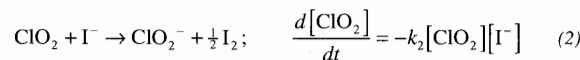
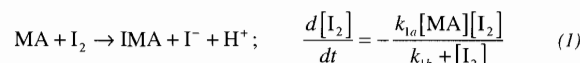
then a pitchfork bifurcation occurs at the nonhyperbolic periodic orbit Γ_0 at the bifurcation value $\mu = \mu_0$.

Remark 2. Under the conditions (3) in Theorem 1, the periodic orbit Γ_0 is a multiple limit cycle of multiplicity $m = 2$ and exactly two limit cycles bifurcate from the semi-stable limit cycle Γ_0 as μ varies from μ_0 in one sense or the other. In particular, if $D^2P(0, \mu_0)$ and $P_\mu(0, \mu_0)$ have opposite signs, then there are two limit cycles near Γ_0 for all sufficiently small $\mu - \mu_0 > 0$ and if $D^2P(0, \mu_0)$ and $P_\mu(0, \mu_0)$ have the same sign, then there are two limit cycles near Γ_0 for all sufficiently small $\mu_0 - \mu > 0$.

Chlorine Dioxide–Iodine–Malonic Acid Reaction

The mechanisms of chemical oscillations can be very complex. The BZ reaction is thought to involve more than twenty elementary reaction steps, but luckily many of them equilibrate rapidly—this allows the kinetics to be reduced to as few as three differential equations. See Tyson (1985) for this reduced system and its analysis.

In a similar spirit, Lengyel et al. (1990) have proposed and analyzed a particularly elegant model of another oscillating reaction, the chlorine dioxide–iodine–malonic acid (ClO_2 – I_2 –MA) reaction. Their experiments show that the following three reactions and empirical rate laws capture the behavior of the system:



Typical values of the concentrations and kinetic parameters are given in Lengyel et al. (1990) and Lengyel and Epstein (1991).

Numerical integrations of (1)–(3) show that the model exhibits oscillations that closely resemble those observed experimentally. However this model is still too complicated to handle analytically. To simplify it, Lengyel et al. (1990) use a result found in their simulations: Three of the reactants (MA, I_2 , and ClO_2) vary much more slowly than the intermediates I^- and ClO_2^- , which change by several orders of magnitude during an oscillation period. By approximating the concentrations of the slow reactants as *constants* and making other reasonable simplifications, they reduce the system to a two-variable model. (Of course, since this approximation neglects the slow consumption of the reactants, the model will be unable to account for the eventual approach to equilibrium.) After suitable nondimensionalization, the model becomes

$$\dot{x} = a - x - \frac{4xy}{1+x^2} \quad (4)$$

$$\dot{y} = bx \left(1 - \frac{y}{1+x^2}\right) \quad (5)$$

where x and y are the dimensionless concentrations of I^- and ClO_2^- . The parameters $a, b > 0$ depend on the empirical rate constants and on the concentrations assumed for the slow reactants.

We begin the analysis of (4), (5) by constructing a trapping region and applying the Poincaré–Bendixson theorem. Then we'll show that the chemical oscillations arise from a supercritical Hopf bifurcation.

EXAMPLE 8.3.1:

Prove that the system (4), (5) has a closed orbit in the positive quadrant $x, y > 0$ if a and b satisfy certain constraints, to be determined.

Solution: As in Example 7.3.2, the nullclines help us to construct a trapping region. Equation (4) shows that $\dot{x} = 0$ on the curve

$$y = \frac{(a-x)(1+x^2)}{4x} \quad (6)$$

and (5) shows that $\dot{y} = 0$ on the y -axis and on the parabola $y = 1+x^2$. These nullclines are sketched in Figure 8.3.1, along with some representative vectors.

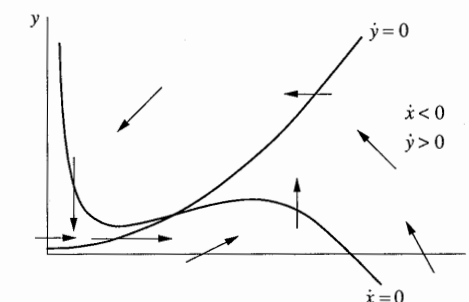


Figure 8.3.1

(We've taken some pedagogical license with Figure 8.3.1; the curvature of the nullcline (6) has been exaggerated to highlight its shape, and to give us more room to draw the vectors.)

Now consider the dashed box shown in Figure 8.3.2. It's a trapping region because all the vectors on the boundary point into the box.

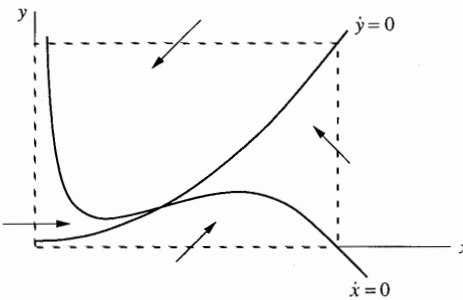


Figure 8.3.2

We can't apply the Poincaré–Bendixson theorem yet, because there's a fixed point

$$x^* = a/5, \quad y^* = 1 + (x^*)^2 = 1 + (a/5)^2$$

inside the box at the intersection of the nullclines. But now we argue as in Example 7.3.3: if the fixed point turns out to be a *repeller*, we *can* apply the Poincaré–Bendixson theorem to the “punctured” box obtained by removing the fixed point.

All that remains is to see under what conditions (if any) the fixed point is a repeller. The Jacobian at (x^*, y^*) is

$$\frac{1}{1+(x^*)^2} \begin{pmatrix} 3(x^*)^2 - 5 & -4x^* \\ 2b(x^*)^2 & -bx^* \end{pmatrix}.$$

(We've used the relation $y^* = 1 + (x^*)^2$ to simplify some of the entries in the Jacobian.) The determinant and trace are given by

$$\Delta = \frac{5bx^*}{1+(x^*)^2} > 0, \quad \tau = \frac{3(x^*)^2 - 5 - bx^*}{1+(x^*)^2}.$$

We're in luck—since $\Delta > 0$, the fixed point is never a saddle. Hence (x^*, y^*) is a repeller if $\tau > 0$, i.e., if

$$b < b_c \equiv 3a/5 - 25/a. \quad (7)$$

When (7) holds, the Poincaré–Bendixson theorem implies the existence of a closed orbit somewhere in the punctured box. ■

EXAMPLE 8.3.2:

Using numerical integration, show that a Hopf bifurcation occurs at $b = b_c$ and

decide whether the bifurcation is sub- or supercritical.

Solution: The analytical results above show that as b decreases through b_c , the fixed point changes from a stable spiral to an unstable spiral; this is the signature of a Hopf bifurcation. Figure 8.3.3 plots two typical phase portraits. (Here we have chosen $a = 10$; then (7) implies $b_c = 3.5$.) When $b > b_c$, all trajectories spiral into the stable fixed point (Figure 8.3.3a), while for $b < b_c$ they are attracted to a stable limit cycle (Figure 8.3.3b).

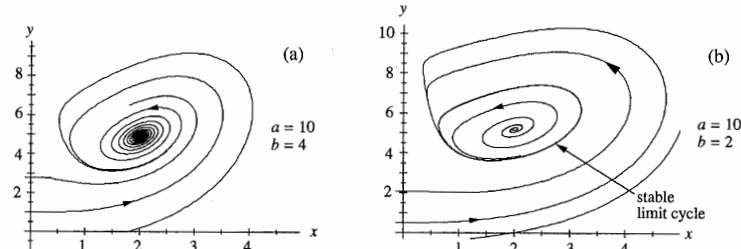


Figure 8.3.3

Hence the bifurcation is *supercritical*—after the fixed point loses stability, it is surrounded by a stable limit cycle. Moreover, by plotting phase portraits as $b \rightarrow b_c$ from below, we could confirm that the limit cycle shrinks continuously to a point, as required. ■

Our results are summarized in the stability diagram in Figure 8.3.4. The boundary between the two regions is given by the Hopf bifurcation locus $b = 3a/5 - 25/a$.

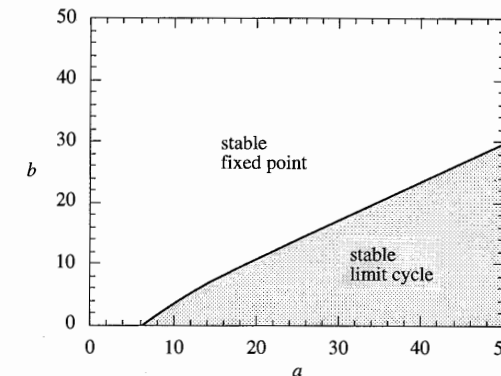


Figure 8.3.4

EXAMPLE 8.3.3:

Approximate the period of the limit cycle for b slightly less than b_c .

Solution: The frequency is approximated by the imaginary part of the eigenvalues at the bifurcation. As usual, the eigenvalues satisfy $\lambda^2 - \tau\lambda + \Delta = 0$. Since $\tau = 0$ and $\Delta > 0$ at $b = b_c$, we find

$$\lambda = \pm i\sqrt{\Delta}.$$

But at b_c ,

$$\Delta = \frac{5b_c x^*}{1+(x^*)^2} = \frac{5\left(\frac{3a}{5} - \frac{25}{a}\right)\left(\frac{a}{5}\right)}{1+(a/5)^2} = \frac{15a^2 - 625}{a^2 + 25}.$$

Hence $\omega \approx \Delta^{1/2} = [(15a^2 - 625)/(a^2 + 25)]^{1/2}$ and therefore

$$\begin{aligned} T &= 2\pi/\omega \\ &= 2\pi[(a^2 + 25)/(15a^2 - 625)]^{1/2}. \end{aligned}$$

A graph of $T(a)$ is shown in Figure 8.3.5. As $a \rightarrow \infty$, $T \rightarrow 2\pi/\sqrt{15} \approx 1.63$. ■

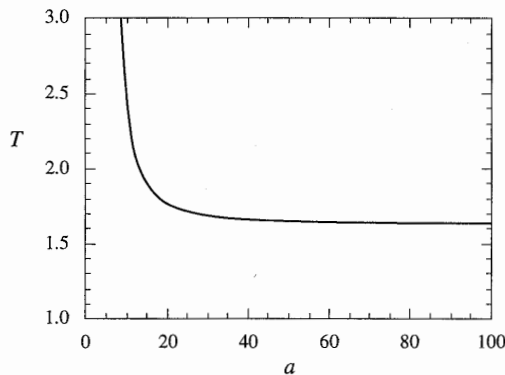


Figure 8.3.5

8.4 Global Bifurcations of Cycles

In two-dimensional systems, there are four common ways in which limit cycles are created or destroyed. The Hopf bifurcation is the most famous, but the other three deserve their day in the sun. They are harder to detect because they involve large

regions of the phase plane rather than just the neighborhood of a single fixed point. Hence they are called *global bifurcations*. In this section we offer some prototypical examples of global bifurcations, and then compare them to one another and to the Hopf bifurcation. A few of their scientific applications are discussed in Sections 8.5 and 8.6 and in the exercises.

Saddle-node Bifurcation of Cycles

A bifurcation in which two limit cycles coalesce and annihilate is called a *fold* or *saddle-node bifurcation of cycles*, by analogy with the related bifurcation of fixed points. An example occurs in the system

$$\begin{aligned} \dot{r} &= \mu r + r^3 - r^5 \\ \dot{\theta} &= \omega + br^2 \end{aligned}$$

studied in Section 8.2. There we were interested in the subcritical Hopf bifurcation at $\mu = 0$; now we concentrate on the dynamics for $\mu < 0$.

It is helpful to regard the radial equation $\dot{r} = \mu r + r^3 - r^5$ as a one-dimensional system. As you should check, this system undergoes a saddle-node bifurcation of fixed points at $\mu_c = -1/4$. Now returning to the two-dimensional system, these fixed points correspond to circular *limit cycles*. Figure 8.4.1 plots the “radial phase portraits” and the corresponding behavior in the phase plane.

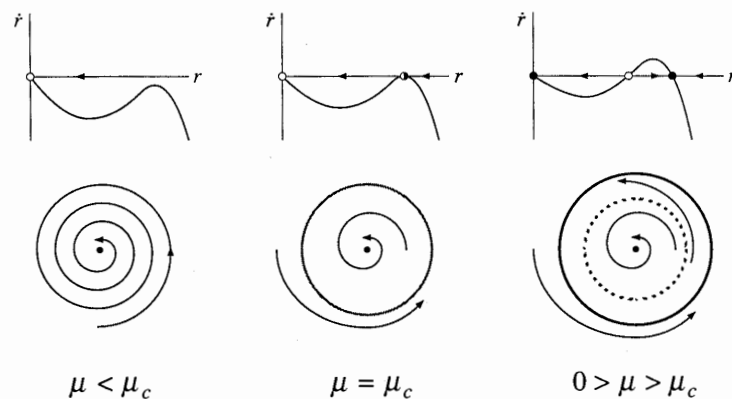


Figure 8.4.1

At μ_c a half-stable cycle is born out of the clear blue sky. As μ increases it splits into a pair of limit cycles, one stable, one unstable. Viewed in the other direction, a stable and unstable cycle collide and disappear as μ decreases through μ_c . Notice that the origin remains stable throughout; it does not participate in this bifurcation.

For future reference, note that at birth the cycle has $O(1)$ amplitude, in contrast to the Hopf bifurcation, where the limit cycle has small amplitude proportional to $(\mu - \mu_c)^{1/2}$.

Infinite-period Bifurcation

Consider the system

$$\begin{aligned}\dot{r} &= r(1 - r^2) \\ \dot{\theta} &= \mu - \sin \theta\end{aligned}$$

where $\mu \geq 0$. This system combines two one-dimensional systems that we have studied previously in Chapters 3 and 4. In the radial direction, all trajectories (except $r^* = 0$) approach the unit circle monotonically as $t \rightarrow \infty$. In the angular direction, the motion is everywhere counterclockwise if $\mu > 1$, whereas there are two invariant rays defined by $\sin \theta = \mu$ if $\mu < 1$. Hence as μ decreases through $\mu_c = 1$, the phase portraits change as in Figure 8.4.2.

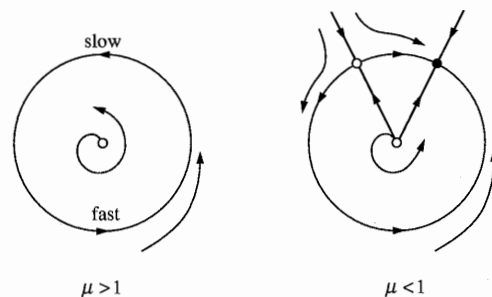


Figure 8.4.2

As μ decreases, the limit cycle $r = 1$ develops a bottleneck at $\theta = \pi/2$ that becomes increasingly severe as $\mu \rightarrow 1^+$. The oscillation period lengthens and finally becomes infinite at $\mu_c = 1$, when a fixed point appears on the circle; hence the term **infinite-period bifurcation**. For $\mu < 1$, the fixed point splits into a saddle and a node.

As the bifurcation is approached, the amplitude of the oscillation stays $O(1)$ but the period increases like $(\mu - \mu_c)^{-1/2}$, for the reasons discussed in Section 4.3.

Homoclinic Bifurcation

In this scenario, part of a limit cycle moves closer and closer to a saddle point. At the bifurcation the cycle touches the saddle point and becomes a homoclinic or-

bit. This is another kind of infinite-period bifurcation; to avoid confusion, we'll call it a *saddle-loop* or *homoclinic bifurcation*.

It is hard to find an analytically transparent example, so we resort to the computer. Consider the system

$$\begin{aligned}\dot{x} &= y \\ \dot{y} &= \mu y + x - x^2 + xy.\end{aligned}$$

Figure 8.4.3 plots a series of phase portraits before, during, and after the bifurcation; only the important features are shown.

Numerically, the bifurcation is found to occur at $\mu_c \approx -0.8645$. For $\mu < \mu_c$, say $\mu = -0.92$, a stable limit cycle passes close to a saddle point at the origin (Figure 8.4.3a). As μ increases to μ_c , the limit cycle swells (Figure 8.4.3b) and bangs into the saddle, creating a homoclinic orbit (Figure 8.4.3c). Once $\mu > \mu_c$, the saddle connection breaks and the loop is destroyed (Figure 8.4.3d).

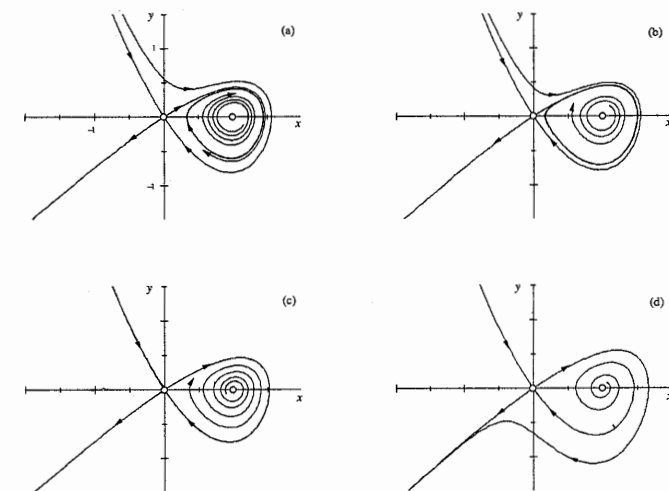


Figure 8.4.3

The key to this bifurcation is the behavior of the unstable manifold of the saddle. Look at the branch of the unstable manifold that leaves the origin to the northeast: after it loops around, it either hits the origin (Figure 8.4.3c) or veers off to one side or the other (Figures 8.4.3a, d).